Electronic Supplementary Material (ESI) for Sustainable Energy & Fuels.

Supporting Information

Salicylic acid treated $Li_7La_3Zr_2O_{12}$ achieves dual functions for PEO-based solid polymer electrolyte in lithium metal batteries

Wen He[a], Hui Ding[a], Chuandong Li[a], Xu Chen [a], Wensheng Yang [*,a]

[a] *State Key Laboratory of Chemical Resource Engineering, Beijing University of Chemical Technology, Beijing 100029, P. R. China*

Experimental section

Synthesis of LLZO powder

LLZO was prepared by a simple sol-gel process. $LiOH \cdot H_2O$, $La(NO_3)_3 \cdot 6H_2O$, and $ZrO(NO_3)_2 \cdot xH_2O$ (All purchased from Aladdin, Shanghai, China) were weighed to reach the intended stoichiometry with an excess of 10wt% $LiOH \cdot H_2O$. Then dissolve them in deionized water with stirring at 80°C. Citric acid was then added to the abovementioned solution at a citric acid to cation molar ratio of 4:1. After dissolution, the obtained homogeneous solution was heated at 80°C for 12 h with magnetic stirring to evaporate the solvent. The product was then dried at 250°C for 2 h and gradually formed a tawny gel. The obtained precursor was ground and calcinated at 700°C for 5 h in air. Finally, the LLZO particles were ball milled to obtain nano-level particles.

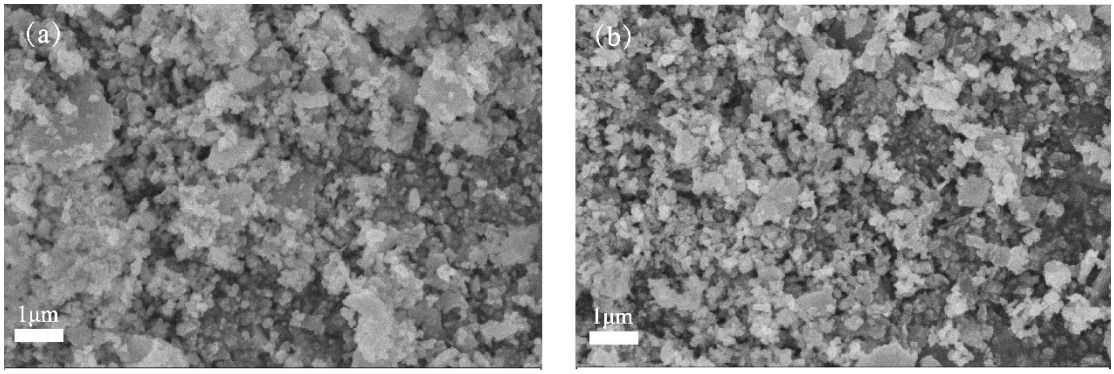

Fig. S1 SEM image of (a) LLZO-air and (b) 7%SA/LLZO.

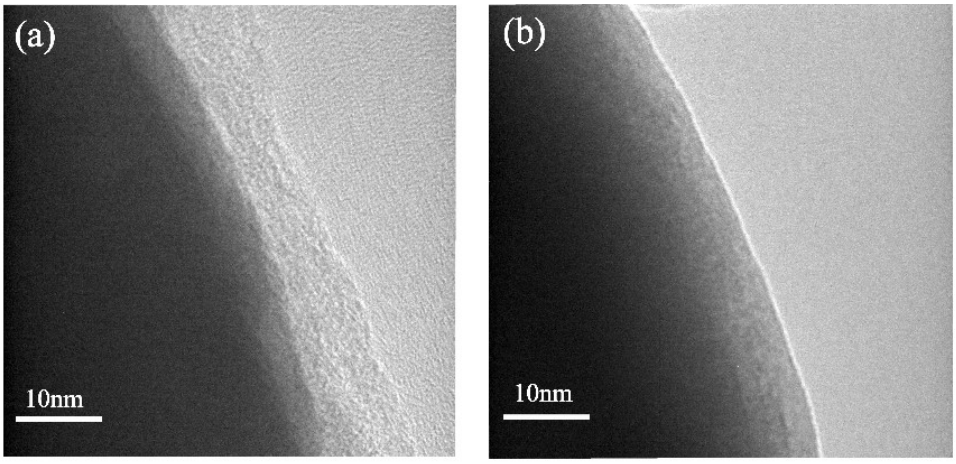

Fig. S2 a-b) HRTEM image of LLZO-air and 7%SA/LLZO particles.

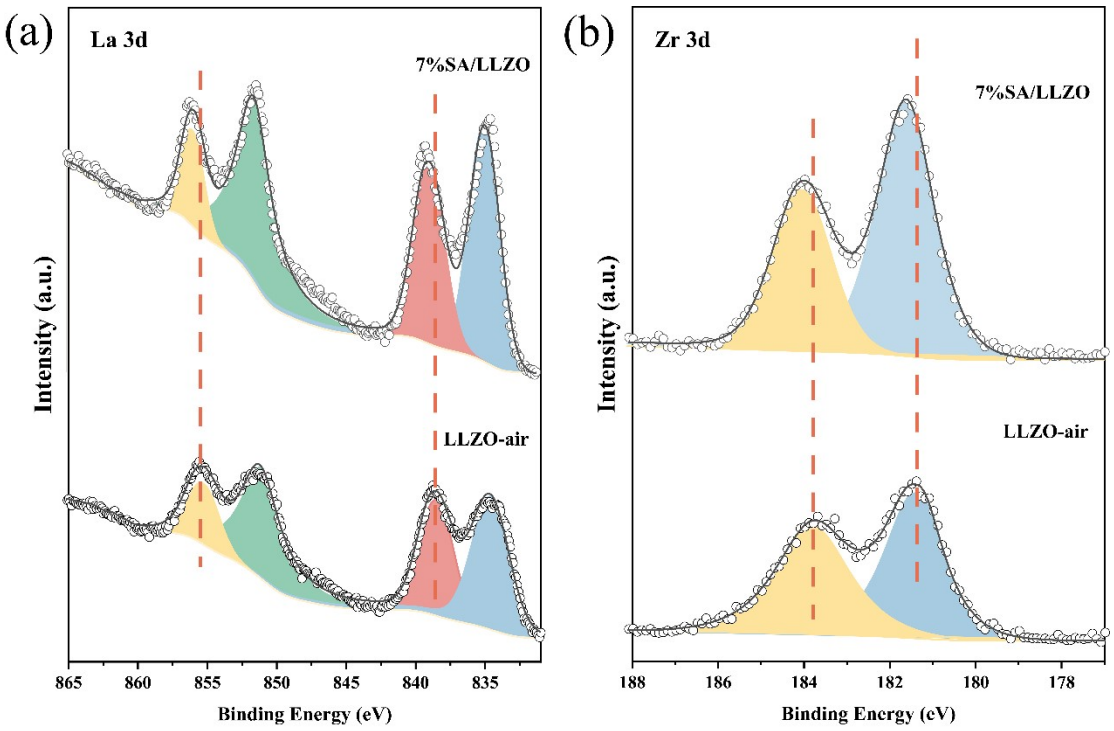

Fig. S3 XPS results of (a) La and (b) Zr of LLZO-air and 7%SA/LLZO.

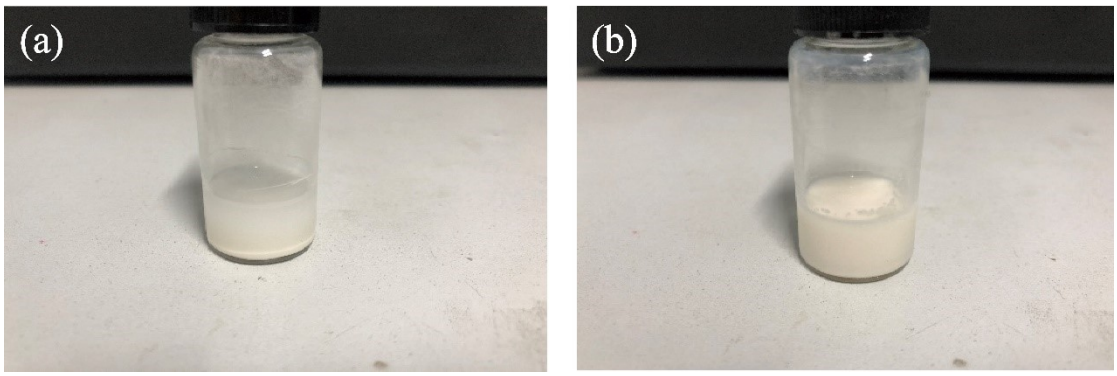

Fig. S4 Photographs of mixed slurry after standing for 24h of (a) LLZO-air-PEO-LiTFSI, (b) 7%SA/LLZO-PEO-LiTFSI.

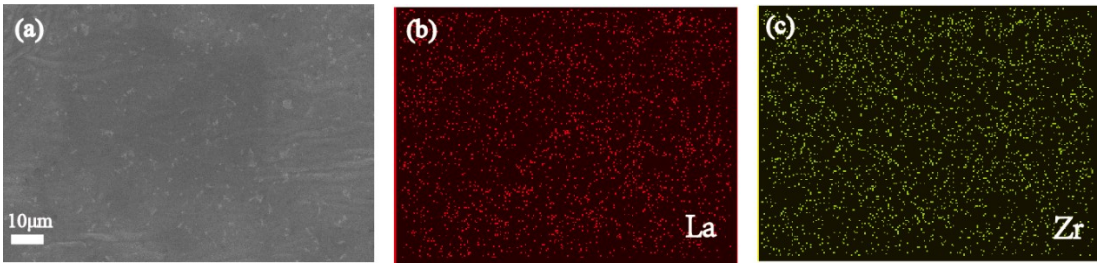

Fig. S5 SEM image of 7%SA/LLZO-PEO-LiTFSI PGE and corresponding EDX maps of La and Zr elements.

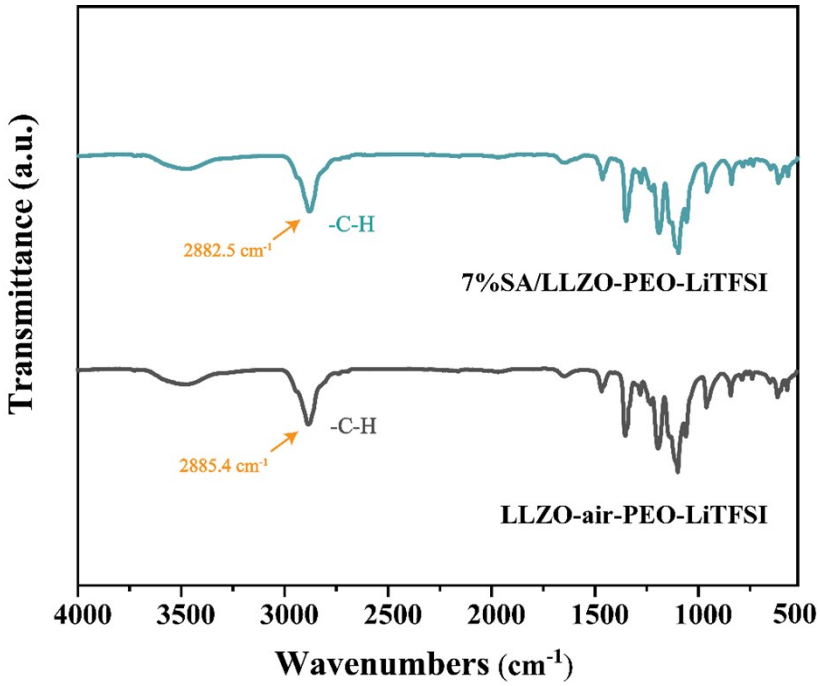

Fig. S6 The FTIR spectra of LLZO-air-PEO-LiTFSI and 7%SA/LLZO-PEO-LiTFSI.

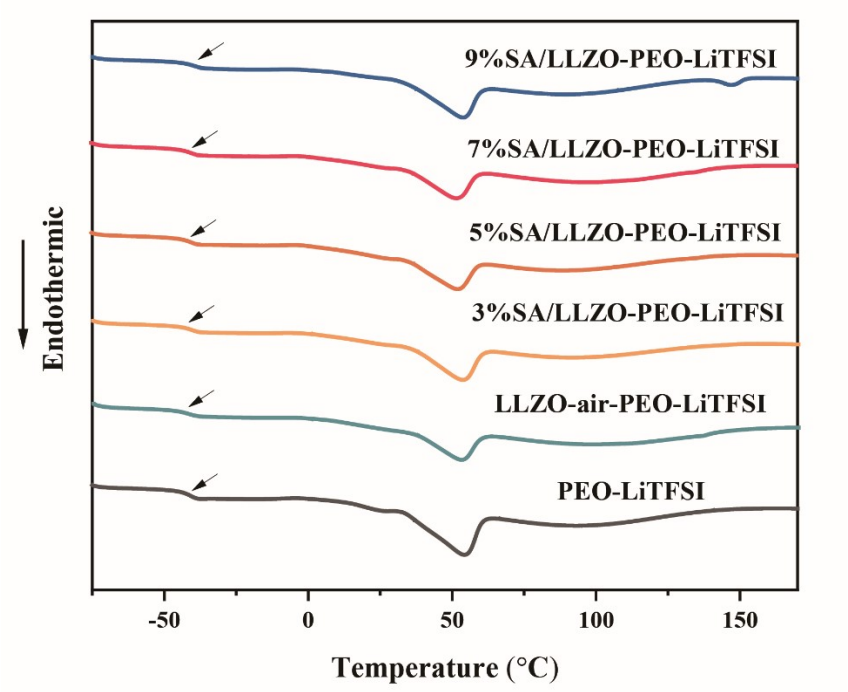

Fig. S7 DSC profiles of different X%SA/LLZO-PEO-LiTFSI PGEs.

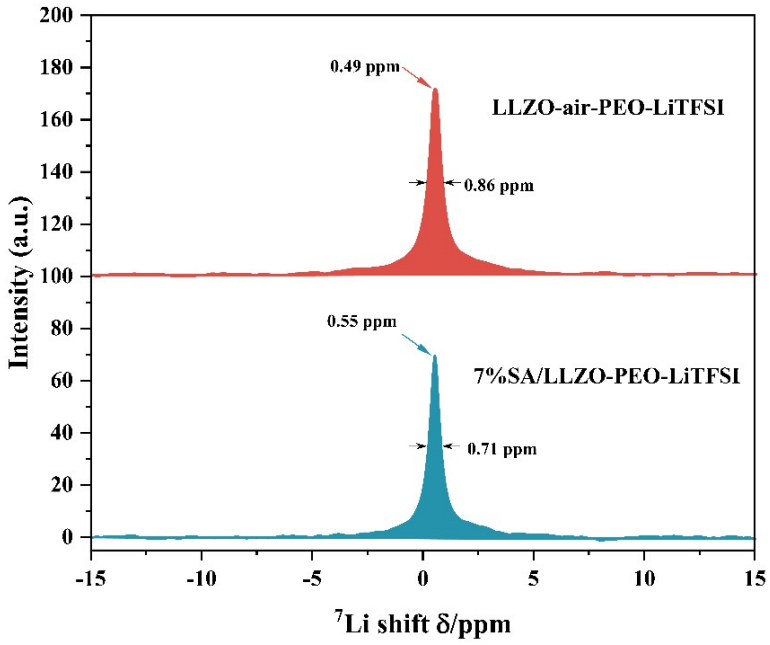

Fig. S8 ^{7}Li solid-state NMR spectra of LLZO-air-PEO-LiTFSI and 7%SA/LLZO-PEO-LiTFSI.

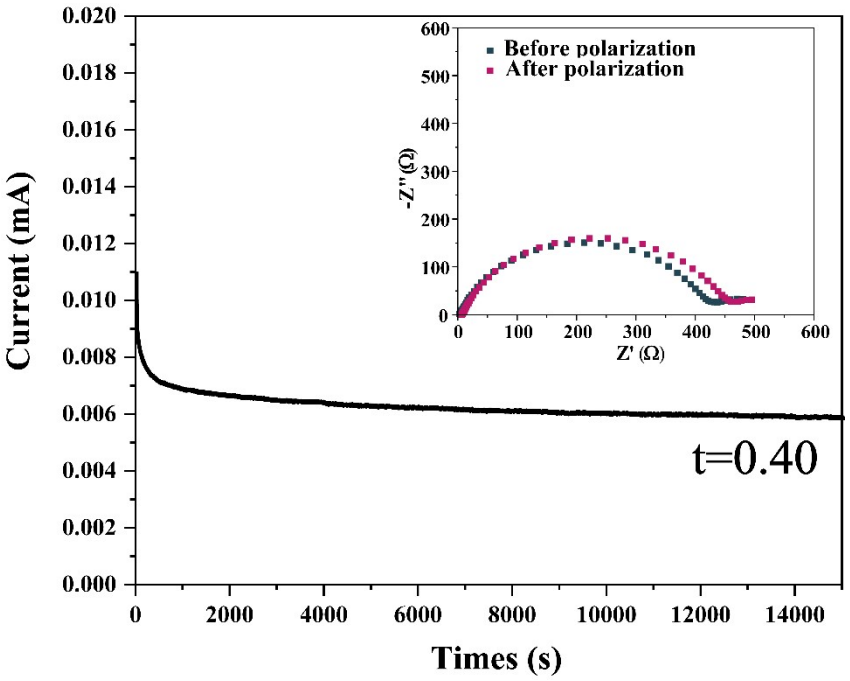

Fig. S9 DC polarization curve of LLZO-air-PEO-LiTFSI obtained from chronoamperometry with an applied polarization voltage of 10 mV and the inset shows the Nyquist profiles of the symmetric battery before and after polarization.

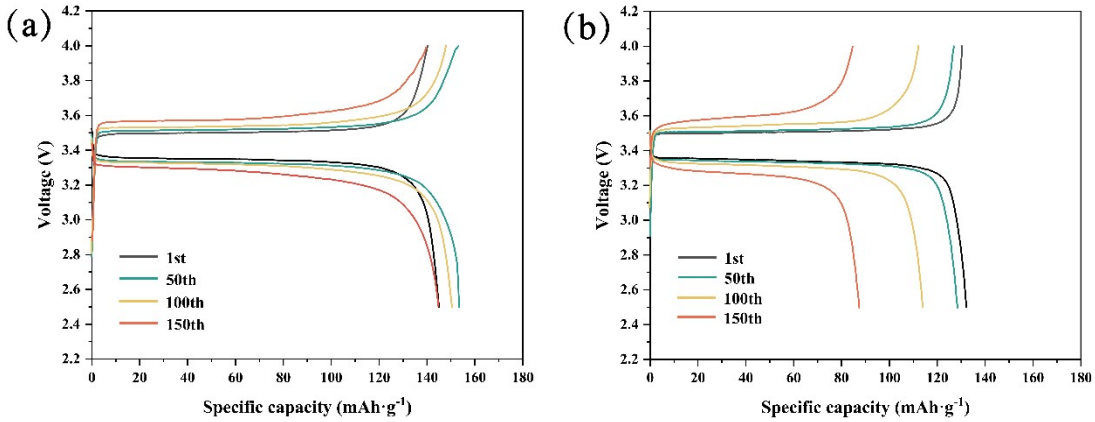

Fig.S10 Charge/discharge curves of a) Li/7%SA/LLZO-PEO-LiTFSI/LFP and b) Li/LLZO-air-PEO-LiTFSI/LFP under 0.3 C.

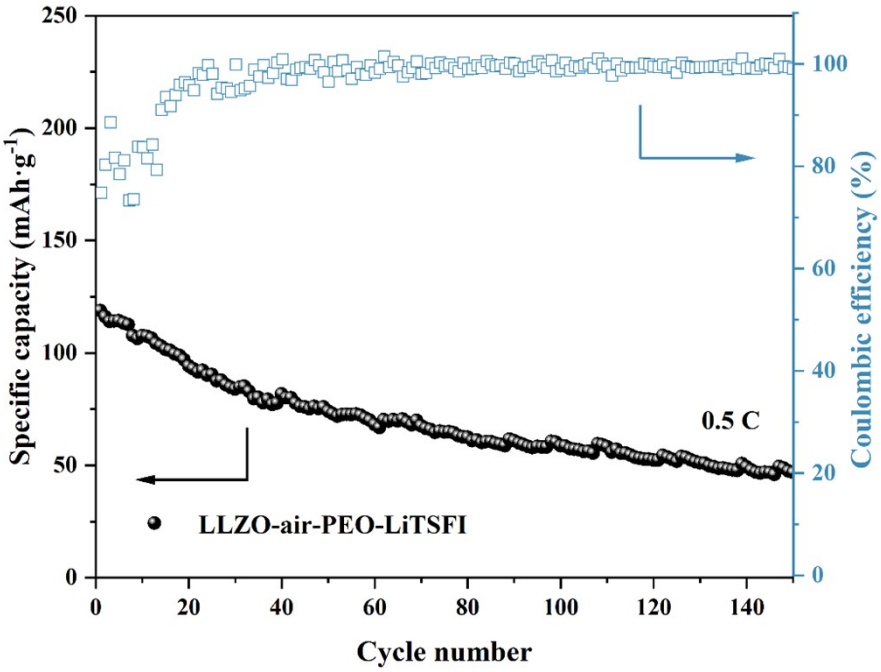

Fig.S11 Cycling performances of Li/LLZO-air-PEO-LiTFSI/LFP at 0.5 C.

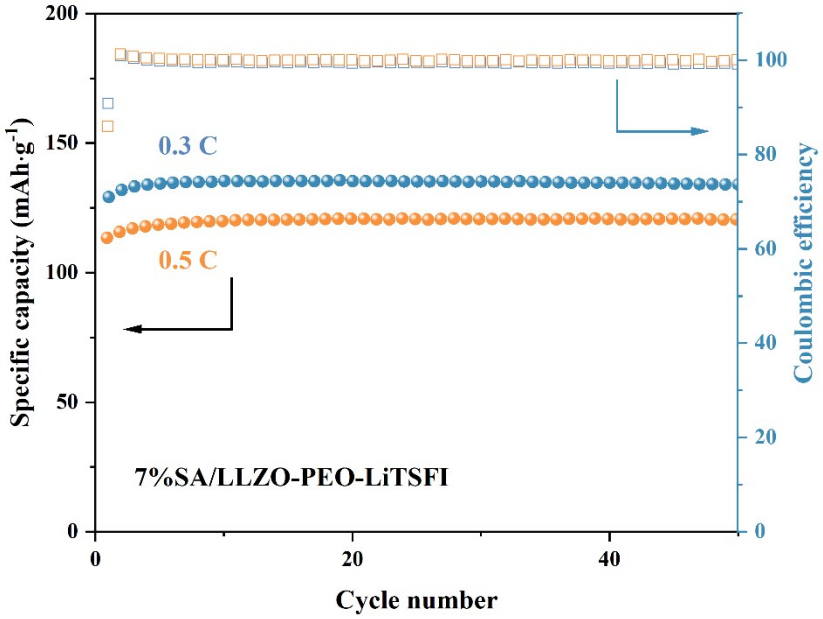

Fig.S12 Cycling performances of Li/7%SA/LLZO-PEO-LiTFSI /LFP at different rate (the mass loading of LFP was 18.2 mg·cm^{-2}).

Table S1 Comparison of Li|PGEs|$LiFePO_4$ batteries with different methods to remove Li_2CO_3 from the surface of LLZO.

Method, composition	Ionic conductivity ($S \cdot cm^{-1}$)	Stability with Li	Cell performance	Reference
High-temperature treatment(600°C) LLZO/PEO solid state electrolyte	3.4×10^{-5} $S \cdot cm^{-1}$ at 25 °C	600 h at 0.2 $mA \cdot cm^{-2}$	Coupled with LFP After 200 cycles at 0.1C, remained 125.3 $mAh \cdot g^{-1}$ at 60°C	1
HCl treatment LLZTO/PEO Quasi-solid state electrolyte	2.2×10^{-4} $S \cdot cm^{-1}$ at 25 °C	400 h at 0.2 $mA \cdot cm^{-2}$	Coupled with LFP After 150 cycles at 0.5C, remained 154.8 $mAh \cdot g^{-1}$ at 60°C	2
Dopamine coating LLZO/PEO solid state electrolyte	1×10^{-4} $S \cdot cm^{-1}$ at 25 °C	600 h at 0.1 $mA \cdot cm^{-2}$	Coupled with LFP After 100 cycles at 0.1C, remained 134.8 $mAh \cdot g^{-1}$ at 25°C	3
Al–Ta and Al–Nb doped LLZO solid state electrolyte	--	80 h at 0.1 $mA \cdot cm^{-2}$ at 55 °C	--	4
reacting garnet with carbon at 700 °C LLZO solid state electrolyte	--	450 h at 0.1 $mA \cdot cm^{-2}$ at 65 °C	Coupled with LFP After 50 cycles at 0.1/0.2C, remained 143 $mAh \cdot g^{-1}$ at 65°C	5
Salicylic treatment LLZO/PEO solid state electrolyte	1.2×10^{-4} $S \cdot cm^{-1}$ at 30 °C	1300 h at 0.1/0.2 $mA \cdot cm^{-2}$	Coupled with LFP After 150 cycles at 0.3C, remained 142.8 $mAh \cdot g^{-1}$ at 40°C	**This work**

Note: In this work, the Li|$LiFePO_4$ battery exhibits higher discharge capacity and capacity retention after cycling at a larger rate, and the operating temperature of the battery is lower than other works. Our work has an advantageous overall performance.

1. H. Huo, X. Li, Y. Sun, X. Lin, K. Doyle-Davis, J. Liang, X. Gao, R. Li, H. Huang, X. Guo and X. Sun, *Nano Energy*, 2020, **73**, 104836.
2. Y. Guo, J. Cheng, Z. Zeng, Y. Li, H. Zhang, D. Li and L. Ci, *ACS Applied Energy Materials*, 2022, **5**, 2853-2861.
3. M. Jia, Z. Bi, C. Shi, N. Zhao and X. Guo, *Journal of Power Sources*, 2021, **486**.
4. L. Huang, J. Gao, Z. Bi, N. Zhao, J. Wu, Q. Fang, X. Wang, Y. Wan and X. Guo, *Energies*, 2022, **15**.
5. Y. Li, X. Chen, A. Dolocan, Z. Cui, S. Xin, L. Xue, H. Xu, K. Park and J. B. Goodenough, *Journal of the American Chemical Society*, 2018, **140**, 6448-6455.